IEEE Access
Multidisciplinary Rapid Review Open Access Journal

Received 5 December 2022, accepted 17 January 2023, date of publication 25 January 2023, date of current version 30 January 2023.

Digital Object Identifier 10.1109/ACCESS.2023.3239665

RESEARCH ARTICLE

H_∞ Control for Oscillator Systems With Event-Triggering Signal Transmission of Internet of Things

LUY NGUYEN TAN [1], **(Member, IEEE), NISHU GUPTA** [2], **(Senior Member, IEEE), AND MOHAMMAD DERAWI** [2]

[1]Faculty of Electrical-Electronics Engineering (FEEE), Ho Chi Minh City University of Technology (HCMUT)—Vietnam National University Ho Chi Minh City (VNU-HCM), Ho Chi Minh City 700000, Vietnam

[2]Department of Electronic Systems, Faculty of Information Technology and Electrical Engineering, Norwegian University of Science and Technology, 2815 Gjøvik, Norway

Corresponding author: Nishu Gupta (nishu.gupta@ntnu.no)

ABSTRACT This article proposes to design a distributed H_∞ optimal control algorithm for Van der Pol oscillators with unknown internal dynamics, input constraints and external disturbances, via event-triggering signal transmission of the Internet of Things (IoT). First, the graph theory for the IoT is introduced. Second, the dynamics of Van der Pol oscillators are transformed into the tracking dynamics which cooperate via the IoT network. Third, unlike the existing online optimal control algorithms using adaptive dynamic programming, we design an H_∞ optimal control algorithm employing an event-triggering signal transmission mechanism to reduce the burden of communication resource and computation bandwidth of the IoT network. As the triggering condition and approximation parameter update policies are appropriately designed, the algorithm guarantees that the Zeno phenomenon is free, the consensus errors are uniformly ultimately bounded, and the external disturbance is compensated. Finally, numerical simulation results with comparison to the time-triggering algorithms confirm the effectiveness of the proposed algorithm.

INDEX TERMS Communication resources, event-triggering, IoT, multi-agent systems, neural network, Van der Pol oscillators.

I. INTRODUCTION

Internet of Things (IoT) technology has recently received significant attention from research communities and industrial societies due to the communication ability among devices and intelligent selection ability of perception and execution [1], [2], [3]. The controller for each device in the IoT can interact through the network to exchange data, generate control signals, and send feedback to others [4], [5], [6], [7], thanks to machine learning, distributed control algorithms for devices/plants that have been widely studied for recent years [6], [7], [8].

The non-IoT conventional distributed control algorithms are based on the time-triggering mechanism, where the controllers sample the states with the same periods and then exchange information with each other through the communication network. This way of transmitting information is inefficient because a device periodically continuously sends the same information to others or its remote controller [9]. To overcome the burden of communication resource and computation bandwidth, the event-triggering mechanism was first investigated for scheduling stabilizing control tasks [10], where a controller only receives feedback states, updates its parameters and sends control signals to plant only when an event-triggering condition is violated. Inspired by the idea, several works related to event-triggered (ET) control for multiagent have been developed [11], [12], [13], [14], [16]. In [11], the ET decentralized control scheme for interconnected nonlinear systems is proposed. The event-triggering condition

The associate editor coordinating the review of this manuscript and approving it for publication was Sathish Kumar.

is designed suitably to reduce the computational burden on the controllers. Narayanan and Jagannathan [12] proposed a distributed optimal control scheme for interconnected affine nonlinear systems, where observers used the triggered system output to estimate the states of the subsystem. Vamvoudakis et.al. [13] designed the ET optimal tracking control algorithm using actor-critic structure in reinforcement learning theory of machine learning. Tan [14] designed an ET H_∞ distributed control algorithm for large-scale systems with physical interconnection, external disturbances and input constraints, where the subsystems are isolated and exchange states and control signals over the network. Qin et.al. [15] proposed a safe ET control method based on ADP and the zero-sum game theory for nonlinear safety-critical systems with safety constraints and input saturation.

However, the algorithms mentioned above, despite using event-triggering mechanisms, are mainly designed for non-IoT-controlled plants, which have the advantages of stable limit cycles and stable equilibrium points at the origin. For example, distributed control algorithms were devoted to consensus problems of the systems with simple models in a kinematic form or a double integrator (see [17] for more details about the applications). An ET control learning algorithm was designed for an application of voltage source inverters in [16], where the disturbance rejection policy and the optimal control policy are approximated to drive the AC output to the reference while minimizing energy loss. Unfortunately, it only applies to single systems that are not connected to the IoT network.

Recently, the Van der Pol oscillators, an original model of an electrical circuit with a triode valve [18], have been interconnected in IoT networks due to the requirement of industrial applications [1, Ch. 6], [19]. The model is then extended to dynamics of relaxation oscillations, elementary bifurcations, and chaos [20], [21], [22], [23]. The different models have been used to design various practical IoT applications in radio engineering, power systems, combustion processes, biomedical engineering, and robotics. In [24], [25], and [26], Van der Pol oscillators, including uncertain parameters and unmodeled dynamics, were controlled by adaptive control algorithms using neural networks (NN). In [27], the outputs of the oscillators were forced to track the reference by NN-based feedback linearizing control algorithms. Experimentally, a sliding-mode observer was used to estimate the states of the oscillators [28]. In optimal control, the oscillators were presented by the strict-feedback nonlinear systems [1, Ch. 6], [29], [30] and nonlinear systems with input constraints [1, Ch. 6], [31]. The optimal control laws were derived from adaptive dynamic programming (ADP) principle.

Although Van der Pol oscillators are widely applied to many engineering disciplines, IoT-based control with the event-triggering signal transmission has not yet been concerned about saving communication resources. Furthermore, the oscillators in the IoT network, impacted by unknown internal dynamics, input constraints and external disturbances, has been not considered. In this paper, the signals of constrained control and disturbance estimation will be exchanged over the IoT network for executing the control policies. The exchange is in the dynamic sampling instants with variable inter-event time rather than fixed sampling periods. These instants are generated by an adaptive event-triggering condition to guarantee closed-loop stability.

Compared with the works mentioned above, the main contributions of this article are three-fold:

1) Unlike the available algorithms of distributed optimal control for nonlinear systems that are not connected to the IoT network [11], [12], [13], [14], [16], we design an algorithm for Van der Pol oscillators in the IoT network dealing with neither controlled stable limit cycles nor stable controllable equilibrium points at the origin. Especially, the system model is in the presence of unknown internal dynamics, input constraint and external disturbance.
2) Unlike the optimal control methods for the Van der Pol oscillators [1, Ch. 6], [29], [31], we further integrate the event-triggering signal transmission of the IoT to ADP and the two-person zero-sum game theory [32], [33] to obtain a new ET control algorithm which can mitigate the communication resource and computational bandwidth in the IoT network. The ET solution of Hamilton-Jacobi-Isaacs (HJI) is approximated online to find the saddle point for control and disturbance compensation policies. In addition, the difference between the ET control algorithm in the paper and one in [30] is that the distributed control via the IoT network is considered instead of decentralized control through non-IoT-subsystem isolation.
3) An adaptive triggering condition is designed and a rigorous proof is made to ensure that the closed dynamics are asymptotically stable while the Zeno phenomenon is excluded. Compared with the sampling period–based control algorithm in terms of communication resource and computation bandwidth in an application, the proposed algorithm is shown to be more effective.

The rest of the paper is organized as follows. Section I introduces the preliminaries including the graph theory for the IoT and the system dynamics, Section III presents the analysis and designs algorithms, Section IV applies the algorithm in numerical simulation studies, and Section V briefly concludes the paper.

Notation 1: Throughout this article, $X \in \mathbb{R}^n$ denotes vector X with the n-dimensional Euclidean space, and $Y \in \mathbb{R}^{n\times m}$ denotes matrix Y with the $n \times m$-dimensional real space. $\|X\|$ and $\|Y\|$ are the Euclidean norm of X and the L_2-norm of Y, respectively. $\lambda_{\min}(.)$ denotes the minimum eigenvalue of a matrix $(\cdot)$, $\underline{\sigma}(.)$ is the minimum singular value of a matrix (.), and diag$[X]$ transforms vector X into a diagonal matrix.

Definition 1 (Uniformly Ultimately Bounded (UUB) [34]): The equilibrium point x_0 of dynamics $\dot{x} = f(x, u), x \in \mathbb{R}^n$ is said to be UUB in a compact set $\Omega \in \mathbb{R}^n$ if there exists a bound B and a time $T(B, x_0)$ for all $x_0 \in \Omega$ such that $\|x - x_0\| \le B, \forall t > t_0 + T$.

II. PRELIMINARIES AND PROBLEM FORMULATION

A. GRAPH THEORY FOR IoT

A graph $\bar{\mathcal{G}}(\mathcal{V}, \Xi, \mathcal{A})$ in the graph theory is employed to construct an IoT topology of devices/plants, where $\mathcal{V} = \{s_1, \ldots, s_N\}$ is a nodes set, $\Xi \subseteq \mathcal{V} \times \mathcal{V}$ is the edge set, $\mathcal{A} = [\mu_{ij}]$ is a weight matrix. If $\mu_{ij} \notin \Xi$, $\mu_{ij} = 0$, otherwise $\mu_{ij} = 1$. If device/plant j can exchange information to device/plant i, s_j is a neighbor of s_i with $j \in \mathbb{N}_i = \{j : s_j \in \mathcal{V}, (s_i, s_j) \in \Xi\}$. Define the Laplacian matrix $\mathcal{L} = \mathcal{B} - \mathcal{A} \in \mathbb{R}^{N\times N}$, $\mathcal{B} = diag(\beta_i)$, $\beta_i = \sum_{j\in\mathbb{N}_i} \mu_{ij}$. The edges from nodes to the root 0, namely leader, is presented by $\mathcal{C} = diag[\alpha_1, \alpha_2, \ldots, \alpha_N]$. If no edge from i to 0, $\alpha_i = 0$, otherwise $\alpha_i = 1$. If there exists a directed edge between s_i and s_j, $\forall(s_i, s_j) \in \mathcal{V}$, $s_i \neq s_j$, $\mathcal{L}$ and $\mathcal{A}$ are irreducible [35].

B. DYNAMICS OF VAN DER POL OSCILLATORS

In this section, we present the normal dynamics of Van der Pol oscillators, then by a definition of event-triggering signal transmission, the tracking errors are defined via the IoT network.

Consider Van der Pol oscillator dynamics i, presented as a strict-feedback nonlinear system with unknown internal dynamics, input constraint and external disturbance:

$$\begin{cases} \dot{x}_{i,1} = f_{i,1}(x_{i,2}) + k_{i,1}(x_{i,1})d_{i,1} \\ \dot{x}_{i,2} = f_{i,2}(x_{i,3}) + k_{i,2}(x_{i,2})d_{i,2} \\ \vdots \\ \dot{x}_{i,n-1} = f_{i,n-1}(x_{i,n}) + k_{i,n-1}(x_{i,n-1})d_{i,n-1} \\ \dot{x}_{i,n} = -f_{i,n}(x_{i,n}) - \frac{1}{2}f_{i,n}(x_{i,n})\left(1 - f_{i,n}^2(x_{i,n-1})\right) \\ \qquad -f_{i,n}^2(x_{i,n-1})f_{i,n}(x_{i,n}) + g_{i,n}\left(x_{i,1}, \ldots, x_{i,n}\right)u_{i,n} \\ \qquad +k_{i,n}(x_{i,1}, \ldots, x_{i,n})d_{i,n} \end{cases} \tag{1}$$

where $u_i \in \mathbb{R}$ is the control input constrained by $\|u_i\| \le \bar{u}_i$ for a positive constant $\bar{u}_i$. For all $l = 1, \ldots, n$, $x_{i,l} \in \mathbb{R}$ is state available for full feedback, $f_{i,l}(.) \in \mathbb{R}$ is unknown function, $g_{i,n}(.) \in \mathbb{R}$, $k_{i,l}(.) \in \mathbb{R}$, are state-dependent functions, $d_{i,l} \in \mathbb{R}$, is external disturbance. The compact form of dynamics (1) is written as

$$\dot{x}_i = \bar{f}_i(x_i) + \bar{g}_i(x_i)u_i + \bar{k}_i(x_i)d_i \tag{2}$$

where $x_i = [x_{i,1}, x_{i,2}, \ldots, x_{i,n}]^\top \in \mathbb{R}^n$, $\bar{g}_i(x_i) = [0, 0, \ldots, g_{i,n}]^\top \in \mathbb{R}^n$, $\bar{k}_i(x_i) = \mathrm{diag}[k_{i,1}, k_{i,2}, \ldots, k_{i,n}] \in \mathbb{R}^{n\times n}$, $d_i = [d_{i,1}, d_{i,2}, \ldots, d_{i,n}]^\top \in \mathbb{R}^n$,

$$\bar{f}_i(x_i) = \begin{bmatrix} f_{i,1}(x_2) \\ f_{i,2}(x_3) \\ \vdots \\ f_{i,n-1}(x_n) \\ -f_{i,n}(x_{i,n}) - \frac{1}{2}f_{i,n}(x_{i,n})\left(1 - f_{i,n}^2(x_{i,n-1})\right) \\ -f_{i,n}^2(x_{i,n-1})f_{i,n}(x_{i,n}) \end{bmatrix}$$

Note that since $f_{i,l}(.)$, $l = 1, \ldots, n$, is unknown, internal dynamics $\bar{f}_i(x_i)$ is completely unknown. To facilitate the later design, we adopt the following assumption.

Assumption 1: $\bar{g}_i(x_i)$ and $\bar{k}_i(x_i)$ are bounded for unknown positive constants b_{ig}, k_{ik}, i.e., $\|\bar{g}_i(x_i)\| \le b_{ig}$, $\left\|\bar{k}_i(x_i)\right\| \le b_{ik}$, $d_i \in \mathcal{L}_2[0, \infty)$, $\bar{f}_i(x_i)$ is Lipschitz continuous.

Remark 1: Assumption 1 is practical in many industrial applications [28], [29], [31], where internal dynamics of (1) is Lipschitz and the measured output is bounded. The upper bounds in Assumption 1 are only used to prove stability (see Appendix A) and are not used in the control law.

Consider the dynamics of the leader without disturbance:

$$\begin{cases} \dot{x}_{0,1} = x_{0,2} \\ \dot{x}_{0,2} = x_{0,3} \\ \vdots \\ \dot{x}_{0,n-1} = x_{0,n} \\ \dot{x}_{0,2} = -x_{0,1} - \frac{1}{2}x_{0,2}(1 - x_{0,1}^2) - x_{0,1}^2x_{0,2} + x_{0,1}u_0 \end{cases} \tag{3}$$

where control input u_0 is constrained by $|u_0| \le \bar{u}_0$, $\bar{u}_0 > 0$.

With the event-triggering signal transmission and the topology of IoT, we define the consensus local tracking error among systems i, neighbors j and leader 0, $x_0 = [x_{0,1}, x_{0,2}]^\top$, as

$$\delta_i = \sum_{j\in\mathbb{N}_i} \mu_{ij}(x_i - x_j) + \alpha_i(x_i - x_0) \tag{4}$$

C. IoT-BASED CONSENSUS TRACKING ERRORS

Assume that at $t_k^i \in \mathcal{T}, \mathcal{T} = \{t_0^i, t_1^i, \ldots, t_k^i, t_{k+1}^i, \ldots, |t_0^i < t_1^i < \ldots < t_k^i < t_{k+1}^i < \ldots\}$, the control input of (1) is updated when an triggering condition, to be designed later, is violated. The triggered dynamics of (2) is rewritten as

$$\dot{x}_i = \bar{f}_i(x_i) + \bar{g}_i(x_i)\underline{u}_i + \bar{k}_i(x_i)d_i \tag{5}$$

where $\underline{u}_i$, $i = 1, 2, \ldots, N$, is updated at t_k^i, $k = 0, 1, \ldots$, and held until t_{k+1}^i by the zero-order hold (ZOH).

We define the triggering consensus local tracking error between system i and its neighbors as

$$\underline{\delta}_i = \sum_{j\in\mathbb{N}_i} \mu_{ij}(\underline{x}_i - \underline{x}_j) + \alpha_i(\underline{x}_i - \underline{x}_0) \tag{6}$$

where $\underline{x}_i = x_i(t_k^i)$, $\underline{x}_j = x_j(t_h^j)$, $h = \mathrm{argmin}_{l\in\mathbb{N}_i}\{t - t_l^j : t \ge t_l^j, t \in [t_k^i, t_{k+1}^i)\}$, $\underline{x}_0 = x_0(t_k^0)$. Let $\underline{\delta} = [\underline{\delta}_1^\top, \underline{\delta}_2^\top, \ldots, \underline{\delta}_N^\top]^\top$ and $\underline{x} = [\underline{x}_1^\top, \underline{x}_2^\top, \ldots, \underline{x}_N^\top]^\top \in \mathbb{R}^{Nn}$ be the overall vectors, the triggering consensus global tracking error vector via parameters of the graph $\bar{\mathcal{G}}(\mathcal{V}, \Xi, \mathcal{A})$ is defined as

$$\begin{aligned} \underline{\delta} &= ((\mathcal{L} + \mathcal{C}) \otimes I_n)(\underline{x} - \bar{1}_N \otimes I_n\underline{x}_0 \in \mathbb{R}^{Nn}) \\ &= ((\mathcal{L} + \mathcal{C}) \otimes I_n)\,\underline{e} \end{aligned} \tag{7}$$

where $\otimes$ is the Kronecker product, $\bar{1}_N = [1, \ldots, 1]^\top \in \mathbb{R}^N$, I_n is an identity matrix of size n, $\underline{e} = \underline{x} - \bar{1}_N \otimes I_n\underline{x}_0 \in \mathbb{R}^{Nn}$ is the event-triggered global tracking error.

The constraint of the triggering consensus local tracking error and triggering consensus global tracking error is followed by Lemma 1.

Lemma 1 ([35]): The bounded local tracking error leads to bounded global tracking error if the following inequality is satisfied with the minimum singular value of $\mathcal{L}+\mathcal{C}$, $\underline{\sigma}(\mathcal{L}+\mathcal{C})$:

$$\|\underline{e}\| \leq \|\underline{\delta}\| / \underline{\sigma}(\mathcal{L}+\mathcal{C}) \tag{8}$$

Control Objective: By Lemma 1, the control objective is to design the locally distributed control policy of each system with unknown internal dynamics, input constraints, and external disturbances. The design employs the event-triggering signal transmission of IoT to reduce the burden of communication resources and computation bandwidth.

III. IoT-BASED DISTRIBUTED H_∞ ET CONTROL

In this section, an event-triggering signal transmission cost function is defined and the HJI equation is derived. Then, an online algorithm is designed for approximate control policy and disturbance compensation policy.

Define $\underline{d}_i = d_i(t_k^i) \neq 0, k = 0, 1, \ldots, i = 1, \ldots, N$ is disturbance compensation policy to be designed later. $\underline{u}_{-i} = \underline{u}_j = u_j(t_h^j), j \in \mathbb{N}_i, h = 0, 1, \ldots, \underline{d}_{-i} = \underline{d}_j = d_j(t_h^j), j \in \mathbb{N}_i, h = 0, 1, \ldots \neq 0$, $\underline{\eta}_i(t) = \left[\underline{\delta}_i^\top(t)\, \underline{u}_i^\top(t)\, \underline{u}_{-i}^\top(t)\right]^\top$. Inspired by the work in [37] for H_∞ optimal control with the disturbance compensation, the performance output $\underline{\eta}_i$ is required to be minimized such that the bounded $\mathcal{L}_2$-gain holds the following condition:

$$\begin{aligned}\int_0^\infty \left\|\underline{\eta}_i^2\right\| \mathrm{d}t &= \int_0^\infty \left(\underline{\delta}_i^\top Q_i \underline{\delta}_i + U(\underline{u}_i) + \sum_{j\in\mathbb{N}_i} U(\underline{u}_j)\right) dt \\ &\leq \int_0^\infty \left(\gamma_i^2 \underline{d}_i^\top \underline{d}_i + \gamma_j^2 \sum_{j\in\mathbb{N}_i} \underline{d}_j^\top \underline{d}_j\right) \mathrm{d}t \end{aligned}\tag{9}$$

where Q_i is a positive definite matrix. By expanding the work in [37], there exists an attenuation level, $\gamma_i > 0$, for the bounded $\mathcal{L}_2$-gain condition (9) to be satisfied, $\forall i = 1, \ldots, N$. For constrained input control problems, the nonnegative function $U(\underline{u}_i)$ is selected by evolving from a single system in [31] and [36] as

$$U(\underline{u}_i) = 2\bar{u}_i \int_0^{\underline{u}_i} (\tanh^{-1})^\top (s/\bar{u}_i) R_i \mathrm{d}s \tag{10}$$

where R_i is the main diagonal elements of a positive definite matrix.

Remark 2: The nonnegative function (10) uses the hyperbolic tangent function, which is a one-to-one real-analytic integrable function of class $C^\eta, \eta \geq 1$, used to map $\mathbb{R}$ onto the interval $(-\bar{u}_i, \bar{u}_i)$.

The triggering local consensus performance index function is defined based on [14] as

$$\begin{aligned} J_i\big(\underline{\delta}_i(0), \underline{d}_i, \underline{d}_{-i}, \underline{u}_i, \underline{u}_{-i}\big) &= \int_0^\infty \Big(\underline{\delta}_i^\top Q_i \underline{\delta}_i + U(\underline{u}_i) \\ &+ \sum_{j\in\mathbb{N}_i} U(\underline{u}_j) - \gamma_i^2 \underline{d}_i^\top \underline{d}_i - \gamma_j^2 \sum_{j\in\mathbb{N}_i} \underline{d}_j^\top \underline{d}_j\Big) \mathrm{d}t \end{aligned}\tag{11}$$

Remark 3: In the cost function (11), different from work in [14], the event-triggering signal transmission is employed for not only the ET control policy but aslo the ET disturbance compensation policy.

Let inputs $\underline{u}_i$ and $\underline{d}_i$ be depended on states. Then, the triggering local consensus value function is written as

$$V_i(\underline{\delta}_i) = \int_t^\infty \mathcal{K}_i\big(\underline{\delta}_i, \underline{d}_i, \underline{d}_{-i} \underline{u}_i, \underline{u}_{-i}, \big) \mathrm{d}t \tag{12}$$

where $\mathcal{K}_i = \underline{\delta}_i^\top Q_i \underline{\delta}_i + U(\underline{u}_i) + \sum_{j\in\mathbb{N}_i} U(\underline{u}_j) - \gamma_i^2 \underline{d}_i^\top \underline{d}_i - \gamma_j^2 \sum_{j\in\mathbb{N}_i} \underline{d}_j^\top \underline{d}_j$. By adopting the two-person zero-sum game theory, we introduce the optimal value $V_i^\star(\underline{\delta}_i)$ [38] as

$$V_i^\star(\underline{\delta}_i) = \min_{\underline{u}_i} \max_{\underline{d}_i} J_i(\underline{\delta}_i(0), \underline{d}_i, \underline{d}_{-i}, \underline{u}_i, \underline{u}_{-i}) \tag{13}$$

The saddle point $(\underline{u}_i^\star, \underline{d}_i^\star)$ to (13) exists if the following Nash condition holds [38]

$$\begin{aligned} &\min_{\underline{u}_i} \max_{\underline{d}_i} J_i\big(\underline{\delta}_i(0), \underline{d}_i, \underline{d}_{-i}, \underline{u}_i, \underline{u}_{-i}\big) \\ &\qquad = \max_{\underline{u}_i} \min_{\underline{d}_i} J_i\big(\underline{\delta}_i(0), \underline{d}_i, \underline{d}_{-i}, \underline{u}_i, \underline{u}_{-i}\big) \end{aligned}\tag{14}$$

Applying the ET control laws and ET disturbance compensation policies to dynamics (4), the consensus tracking dynamics is rewritten as

$$\begin{aligned} \dot{\underline{\delta}}_i &= \bar{f}_i(\underline{z}_i) + (\beta_i + \alpha_i)\Big(\bar{g}_i(\underline{x}_i)\underline{u}_i + \bar{k}_i(\underline{x}_i)\underline{d}_i\Big) \\ &\quad - \sum_{j\in\mathbb{N}_i} \mu_{ij}\Big(\bar{g}_j(\underline{x}_j)\underline{u}_j + \bar{k}_j(\underline{x}_j)\underline{d}_j\Big) \end{aligned}\tag{15}$$

where $\bar{f}_i(\underline{z}_i) = \bar{f}_i(\underline{x}_i) + \sum_{j\in\mathbb{N}_i} \mu_{ij}\bar{f}_j(\underline{x}_j)$. Then, we define the Hamiltonian as

$$\begin{aligned} &H_i\big(\underline{\delta}_i, \underline{d}_i, \underline{d}_{-i}, \underline{u}_i, \underline{u}_{-i}\big) = \mathcal{K}_i \\ &\quad + \nabla V_i^{\star\top}\Big(\bar{f}_i(\underline{z}_i) + (\beta_i + \alpha_i)\Big(\bar{g}_i(\underline{x}_i)\underline{u}_i + \bar{k}_i(\underline{x}_i)\underline{d}_i\Big) \\ &\quad - \sum_{j\in\mathbb{N}_i} \mu_{ij}\Big(\bar{g}_j(\underline{x}_j)\underline{u}_j + \bar{k}_j(\underline{x}_j)\underline{d}_j\Big)\Big) \end{aligned}\tag{16}$$

where $\nabla V_i^\star(\underline{\delta}_i) = \partial V_i^\star(\underline{\delta}_i)/\partial \underline{\delta}_i$. Apply the stationary condition to (16), control and disturbance compensation policies are computed as follows:

$$\underline{d}_i^\star = \frac{1}{2\gamma_i^2}(\beta_i + \alpha_i)\bar{k}_i^\top(\underline{x}_i)\nabla V_i^\star(\underline{\delta}_i) \tag{17}$$

$$\underline{u}_i^\star = -\bar{u}_i \tanh(\underline{M}_i^\star),\ \underline{M}_i^\star = \frac{\beta_i + \alpha_i}{2\bar{u}_i} R_i^{-1} \bar{g}_i^\top(\underline{x}_i)\nabla V_i^\star(\underline{\delta}_i) \tag{18}$$

Substituting (18) and (17) to (16) we have the triggered HJI equation:

$$\begin{aligned} &H_i^\star\big(\underline{\delta}_i, \quad \underline{d}_i^\star, \underline{d}_{-i}^\star, \underline{u}_i^\star, \underline{u}_{-i}^\star\big) = \mathcal{K}_i^\star \\ &\quad + \nabla V_i^{\star\top}\Big(\bar{f}_i(\underline{z}_i) + (\beta_i + \alpha_i)\Big(\bar{g}_i(\underline{x}_i)\underline{u}_i^\star + \bar{k}_i(\underline{x}_i)\underline{d}_i^\star\Big) \\ &\quad - \sum_{j\in\mathbb{N}_i} \mu_{ij}\Big(\bar{g}_j(\underline{x}_j)\underline{u}_j^\star + \bar{k}_j(\underline{x}_j)\underline{d}_j^\star\Big)\Big) = 0 \end{aligned}\tag{19}$$

where $\mathcal{K}_i^\star = \underline{\delta}_i^\top Q_i \underline{\delta}_i + U(\underline{u}_i^\star) + \sum_{j\in\mathbb{N}_i} U(\underline{u}_j^\star) - \gamma_i^2 \underline{d}_i^{\star\top}\underline{d}_i^\star - \gamma_j^2 \sum_{j\in\mathbb{N}_i} \underline{d}_j^{\star\top}\underline{d}_j^\star$.

According to [37], there exists a positive definite smooth minimum solution $V_i^\star(\underline{\delta}_i)$ to the triggered HJI (19). However, as $\bar{f}_i(\underline{z}_i)$ is unknown and (19) is high-order nonlinear differential, the analytical solution cannot be found. NN combined with event-triggering is our choice to learn the solution. The smooth optimal value function $V_i^\star(\underline{\delta}_i)$, $i = 1, \ldots, N$, is therefore approximated by the Weierstrass higher-order approximation theorem [36] as

$$V_i^\star(\underline{\delta}_i) = W_i^\top \phi_i(\underline{\delta}_i) + \varepsilon_i(\underline{\delta}_i) \tag{20}$$

where $\phi_i(\underline{\delta}_i) : \mathbb{R}^n \to \mathbb{R}^h$, W_i and ε_i are the activation functions, the ideal weights and the NN approximation errors, respectively. By the higher-order approximation property we have the following assumption [39].

Assumption 2: If $\phi_i(\underline{\delta}_i)$ is a complete independent basis set, then $\varepsilon_i(\underline{\delta}_i) \to 0$ and $\nabla\varepsilon_i(\underline{\delta}_i) \to 0$ when $h \to \infty$. If h is a finite number, $\|\varepsilon_i(\underline{\delta}_i)\| \le b_{i\varepsilon}$, $\|\nabla\varepsilon_i(\underline{\delta}_i)\| \le b_{i\nabla\varepsilon}$, where $b_{i\varepsilon}$, $b_{i\nabla\varepsilon}$ are positive constants.

We obtain the NN-based triggered HJI by substituting (20) to (18)–(19):

$$\begin{aligned} &H_i^\star\Big(\underline{\delta}_i, W_i^\top\nabla\phi_i, \underline{u}_i^\star, \underline{d}_i^\star\Big) \\ &= \mathcal{K}_i^\star + W_i^\top\nabla\phi_i(\underline{\delta}_i)\Big(\bar{f}_i(\underline{z}_i) + (\beta_i+\alpha_i)\Big(\bar{g}_i(\underline{x}_i)\underline{u}_i^\star + \bar{k}_i(\underline{x}_i)\underline{d}_i^\star\Big) \\ &\qquad - \sum_{j\in\mathbb{N}_i}\mu_{ij}\Big(\bar{g}_j(\underline{x}_j)\underline{u}_j^\star + \bar{k}_j(\underline{x}_j)\underline{d}_j^\star\Big)\Big) - \varepsilon_{iH} = 0 \end{aligned} \tag{21}$$

where

$$\begin{aligned} \varepsilon_{iH} = H_i^\star - H_i = -\nabla\varepsilon_i^\top\Big(\bar{f}_i(\underline{z}_i) + (\beta_i+\alpha_i)\Big(\bar{g}_i(\underline{x}_i)\underline{u}_i^\star \\ +\bar{k}_i(\underline{x}_i)\underline{d}_i^\star\Big) - \sum_{j\in\mathbb{N}_i}\mu_{ij}\Big(\bar{g}_j(\underline{x}_j)u_j^\star + \bar{k}_j(\underline{x}_j)\underline{d}_j^\star\Big)\Big) \end{aligned} \tag{22}$$

Remark 4: Recall Assumption 2 we have the boundedness of ε_{iH} on a compact set, i.e. $\forall b_{iH} > 0$, $\exists N(b_{iH})$: $\sup_{\underline{\delta}_i\in\Omega}\|\varepsilon_{iH}\| \le b_{iH}$. In addition, $\|\varepsilon_{iH}\| \to 0$ when $h \to \infty$ [36].

Since the ideal NN weights are not available, the value function (20) is estimated by

$$\hat{V}_i = \hat{W}_i^\top \phi_i(\underline{\delta}_i) \tag{23}$$

From (17), (18) and (23), the disturbance compensation policy and the optimal control policy are approximated by

$$\underline{\hat{d}}_i = \frac{1}{2\gamma_i^2}(\beta_i+\alpha_i)\bar{k}_i^\top(\underline{x}_i)\nabla\hat{V}_i \tag{24}$$

$$\underline{\hat{u}}_i = -\bar{u}_i\tanh(\underline{\hat{M}}_i),\ \underline{\hat{M}}_i = \frac{1}{2\bar{u}_i}(\beta_i+\alpha_i)R_i^{-1}\bar{g}_i^\top(\underline{x}_i)\nabla\hat{V}_i \tag{25}$$

Using (24), (25) for (21), one obtains the approximate Hamilton as

$$\begin{aligned} \hat{H}_i(\underline{\delta}_i, \hat{W}_i) = \hat{\mathcal{K}}_i + \hat{W}_i^\top\nabla\phi_i(\underline{\delta}_i)\Big(\bar{f}_i(\underline{z}_i) + (\beta_i+\alpha_i) \\ \Big(\bar{g}_i(\underline{x}_i)\underline{\hat{u}}_i + \bar{k}_i(\underline{x}_i)\underline{\hat{d}}_i\Big) - \sum_{j\in\mathbb{N}_i}\mu_{ij}\Big(\bar{g}_j(\underline{x}_j)\underline{\hat{u}}_j + \bar{k}_j(\underline{x}_j)\underline{\hat{d}}_j\Big)\Big) \end{aligned} \tag{26}$$

where $\hat{\mathcal{K}}_i = U(\underline{\hat{u}}_i) + \sum\limits_{j\in\mathbb{N}_i} U(\underline{\hat{u}}_j) - \gamma_i^2\underline{\hat{d}}_i^\top\underline{\hat{d}}_i - \gamma_j^2\sum\limits_{j\in\mathbb{N}_i}\underline{\hat{d}}_j^\top\underline{\hat{d}}_j$.

Next, we propose a NN-weight tuning law to force $\hat{W}_i \to W_i$ for all $i = 1, \ldots, N$. In other words, our goal is to obtain $\hat{H}_i \to H_i^\star \equiv 0$. To remove the system identification procedure for internal dynamics $\bar{f}_i(\underline{z}_i)$, the integrated reinforcement learning technique [40] is used in the paper, i.e., the residual error function, which we establish to minimize, is $E_{i,\hat{H}} = \frac{1}{2}\psi_i^\top\psi_i$,

$$\psi_i = \int_{t-T}^{t} \hat{H}_i\Big(\underline{\delta}_i, \hat{W}_i\Big)\mathrm{d}\tau \tag{27}$$

where $T > 0$ is a small interval. To ensure the NN-weights converge to global values but avoid using the persistent excitation (PE) condition in adaptive control [41], we follow the concurrent learning technique [42]. The total integral past residual error, $E_{i,P} = \sum_{l=1}^{P_i} E_{i,\hat{H}}(t_l)$, is utilized. Then, the NN-weight tuning law is derived from modifying the Levenberg-Marquardt algorithm, such that $\dot{\hat{W}}_i = -\rho_i\frac{\Delta\phi_i}{(\Delta\phi_i^\top\Delta\phi_i+1)^2}\partial E_{i,\hat{H}}/\partial\hat{W}_i - \rho_i\sum_{l=1}^{P_i}\frac{\Delta\phi_i(t_l)}{(\Delta\phi_i(t_l)^\top\Delta\phi_i(t_l)+1)^2}\partial E_{i,P}/\partial\hat{W}_i$

$$\begin{aligned} \Rightarrow \dot{\hat{W}}_i = -\rho_i\frac{\Delta\phi_i}{(\Delta\phi_i^\top\Delta\phi_i+1)^2}\Big(\Delta\phi_i^\top\hat{W}_i + \int_{t-T}^{t}\hat{\mathcal{K}}_i(\tau)\mathrm{d}\tau \\ -\rho_i\sum_{l=1}^{P_i}\Delta\phi_i(t_l)\Big(\Delta\phi_i^\top(t_l)\hat{W}_i + \int_{t_l-T}^{t_l}\hat{\mathcal{K}}_i(\tau)\mathrm{d}\tau\Big)\Big) \end{aligned} \tag{28}$$

where ρ_i is an update rate, and

$$\begin{aligned} \Delta\phi_i(\delta_i(t)) &= \int_{t-T}^{t}\nabla\phi_i\Big(\bar{f}_i(\underline{z}_i) + (\beta_i+\alpha_i)\Big(\bar{g}_i(\underline{x}_i)\underline{\hat{u}}_i \\ &\qquad +\bar{k}_i(\underline{x}_i)\underline{\hat{d}}_i\Big) - \sum_{j\in\mathbb{N}_i}\mu_{ij}\Big(\bar{g}_j(\underline{x}_j)\underline{\hat{u}}_j + \bar{k}_j(\underline{x}_j)\underline{\hat{d}}_j\Big)\Big)\mathrm{d}\tau \\ &= \int_{t-T}^{t}\nabla\phi_i\dot{\delta}_i\mathrm{d}\tau = \phi_i\big(\delta_i(t)\big) - \phi_i(\delta_i(t-T)) \end{aligned} \tag{29}$$

$\Delta\phi_i(\delta_i(t_l))$, $\hat{\mathcal{K}}_i(t_l)$ at $t_l = \{t_0, t_1, \ldots, t_{P_i}\} < t$ are stored in sets $\{\Delta\phi_i(t_l)\}_{l=1}^{P_i}$, $\{\hat{\mathcal{K}}_i\}_{l=0}^{P_i}$. It worth noting that $\{\Delta\phi_i(t_l)\}_{l=0}^{P_i}$ must be linearly independent or $\mathrm{rank}\big[\Delta\phi_1(t_0), \Delta\phi_2(t_1), \ldots, \Delta\phi_i(t_{P_i})\big] = P_i$ [42].

Remark 5: As the unknown internal dynamics, $\bar{f}_i(\underline{z}_i)$, is absent from (29), a system identification procedure for unknown function is unnecessary.

Let the triggering error be defined as $e_i = \delta_i - \underline{\delta}_i$, by the Assumption 2, the following assumption is satisfied:

Assumption 3: For a positive constant $L_{i\nabla\phi}$, $\nabla\phi_i(\underline{\delta}_i)$ is Lipschitz continuous

$$\|\nabla\phi_i(\delta_i) - \nabla\phi_i(\underline{\delta}_i)\| \leq L_{i\nabla\phi}\|\delta_i - \underline{\delta}_i\| = L_{i\nabla\phi}\|e_i\| \tag{30}$$

Next, we design the triggering condition based on the triggering errors and Lyapunov theory. The condition guarantees that the closed- system is stable.

Condition 1 (Event-triggering condition): The consensus tracking errors are sampled and the parameters of disturbance compensation policy and the optimal control policy are updated only when the following triggering condition is violated:

$$\|e_i\| < \left\|e_{iT}\right\| = (1-\kappa_i)\frac{(1-\zeta_i)\lambda_{\min}(Q_i)\left\|\underline{\delta}_i\right\|^2 + U(\underline{\hat{u}}_i) - \gamma_i^2\left\|\underline{\hat{d}}_i\right\|^2}{\left(\frac{1}{\zeta_i}-1\right)\lambda_{\min}(Q_i) + \Lambda_i^2\left\|\hat{W}_i\right\|^2} \tag{31}$$

where $\|e_{iT}\|$ is a triggering threshold, $0 < \zeta_i < 1, 0 \leq \kappa_i < 1$ are design parameters, $\lambda_{\min}(Q_i)$ is the smallest eigenvalue of Q_i, $\Lambda_i^2 = \bar{u}_i^2 b_{ig}^2 L_{i\nabla\phi}^2\|R_i^{-1}\|$.

The IoT-based ET robust optimal control structure for each system is presented in Fig. 1. In the structure, all systems exchange the states, control and disturbance compensation signals over the network. Each system updates the policy parameters only when the triggering gates are enabled. t_k^i or t_h^j are governed by the triggering conditions. The parameters of the disturbance compensation policy and the optimal control policy are adjusted via NN outputs while the NN-weights are adjusted by the online weight tuning law. It is worth emphasizing that all consensus tracking errors are sampled non-periodically.

Remark 6: Although states $\delta_j, j \in \mathbb{N}_i$ are continuously transferred though the network for system i to compute the triggering error e_i, the control signals and disturbance compensation signals of neighbors j are only transferred when the triggering condition 1 is violated, otherwise they use zero-order hold (ZOH). Compared with the time-triggering mechanism, where the signal is transmitted continuously according to the fixed sampling period, the communication load in the event-triggering mechanism is mitigated.

A. STABILITY ANALYSIS AND ZENO PHENOMENON EXCLUSION

In the following theorem, we analyze the stability and the exclusion of the Zeno phenomenon. The Zeno phenomenon occurs if the minimum inter-event interval is zero, resulting in excessively increasing the cumulative number of events.

Theorem 3.1: Consider the Van der Pol oscillators (1), which are networked with the topology resented by the communication graph $\bar{\mathcal{G}}(\mathcal{V}, \Xi, \mathcal{A})$. Let the consensus tracking errors be defined in (6). Let the ET disturbance compensation policy and the ET distributed optimal control policy be approximated in (25) and (24). Let the triggering threshold be designed in (31). Then, the closed-loop dynamics of each system is stable and the approximation errors are ultimately uniformly bounded (UUB). In addition, the Zeno behavior is excluded since

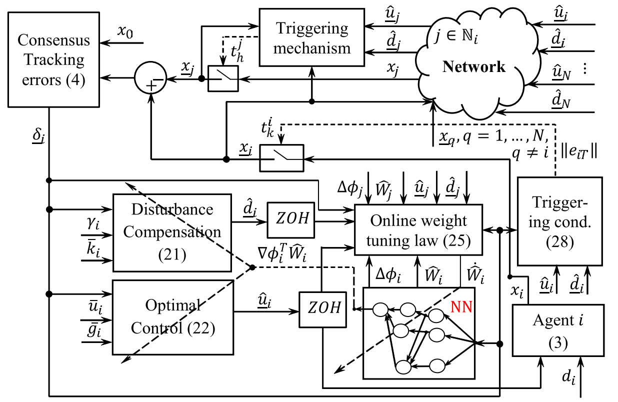

FIGURE 1. **IoT-based ET robust optimal control structure.**

$$t_{\min}^i = \min_k(t_{k+1}^i - t_k^i) \geq \frac{1}{\Gamma_i}\ln\left(1 + \min_{k\in\mathbb{N}}\frac{\left\|e_{iT}(t_{k+1}^{i-})\right\|}{\|\underline{\delta}_i\| + O_i}\right) \tag{32}$$

where Γ_i, O_i are positive upper bounds.

Proof: See Appendix A. ■

Remark 7: In Appendix A, the closed-loop is stable when $\dot{L}_i < -\left((1-\zeta_i)\lambda_{\min}(Q_i)\left\|\underline{\delta}_i\right\|^2 + U(\underline{\hat{u}}_i) - \gamma_i^2\|\underline{\hat{d}}_i\|^2\right) < 0$. It is guaranteed in (31) that $\left\|e_{iT}(t_{k+1}^{i-})\right\| > 0$.

IV. NUMERICAL SIMULATION

In this section, a numerical simulation study of the proposed distributed robust optimal control algorithm for Van der Pol oscillator agents is conducted. The comparison results between the ET control algorithm and the time-triggered (TT) control algorithm [1, Ch. 6] are performed.

The consensus network topology of IoT is presented in Fig. 2, where the leader (a_0), sends its states $\underline{x}_0$ and control signal $\underline{\hat{u}}_0$ to agents 1 and 2 (a_1, a_2). Agent 1 sends its information, including $\underline{x}_1$, control signal $\underline{\hat{u}}_1$, and disturbance compensation signal $\underline{\hat{d}}_1$ to agent 2. Then, agent 1 and agent 2 send their triggered information, including $\underline{x}_1$ and $\underline{x}_2$, control signals $\underline{\hat{u}}_1$ and $\underline{\hat{u}}_2$, and disturbance compensation signals $\underline{\hat{d}}_1$ and $\underline{\hat{d}}_2$, to agent 3 (a_3) at the triggering moments.

The states of the leader is generated by applying the following control law to dynamics (3) with $\bar{u}_0 = 0.1$:

$$\underline{\hat{u}}_0 = -\bar{u}_0\tanh(\underline{\hat{M}}_0),\ \ \underline{\hat{M}}_0 = \frac{1}{2\bar{u}_0}R_0^{-1}\bar{g}_0^\top(\underline{x}_0)\nabla\phi_0^\top(\underline{x}_0)\hat{W}_0$$

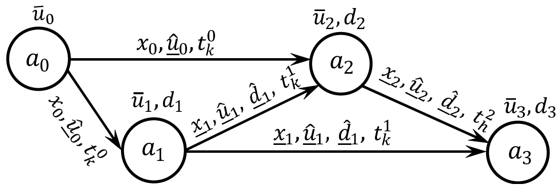

FIGURE 2. Consensus network topology of leader and agents.

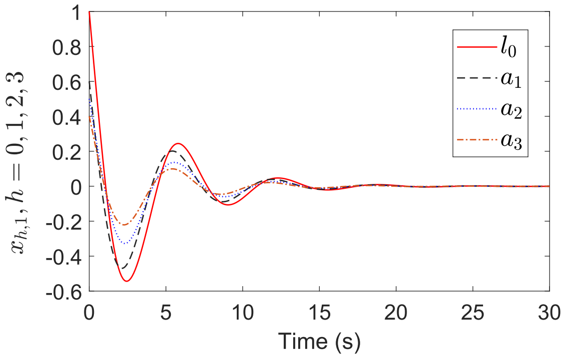

FIGURE 3. Evolution of states of leader and agents for $x_{h,1}, h = 0, \ldots, 3$.

where $\hat{W}_0$ is updated by the law (28) with $\hat{\mathcal{K}}_0 = U(\hat{u}_0)$. The triggering condition of the leader is

$$\|e_0\| < \|e_{0T}\| = (1-\kappa_0)\frac{(1-\zeta_0)\lambda_{\min}(Q_0)\|\underline{x}_0\|^2 + U(\underline{\hat{u}}_0)}{\left(\frac{1}{\zeta_0}-1\right)\lambda_{\min}(Q_0) + \Lambda_0^2\|\hat{W}_0\|^2}$$

The dynamics of all agents are presented in the form of (1), where $\bar{f}_i(x_i) = [x_{i,1}, -x_{i,2} - \frac{1}{2}x_{i,2}(1 - x_{i,1}^2) - x_{i,1}^2 x_{i,2}]^\top$, $\bar{g}_i(x_i) = [0, x_{i,1}]^\top$, $\bar{k}_i(x_i) = \mathrm{diag}[0, 0, \ldots, \sin(4x_{i,1} - 1)x_{i,2}]$. The control input limits $\bar{u}_i = 0.1$. For $h = 0, 1, .., 3$, the initial weights $\hat{W}_h(0) = 0$, $\phi_h = [x_{h,1}^2, x_{h,1}x_{h,2}, x_{h,2}^2]^\top$, $Q_h = I$, $R_h = 0.25$, $\Lambda_h = 0.1$, $\zeta_h = 0.25$, $\kappa_h = 0$, $\gamma_h = 5(h \neq 0)$, the update rates $\rho_h = 25$, the sampling period $T_c = T = 0.1$(s). The dimension of past data $P_h = 20$. In the first 2 seconds, a small probing noise $\sin^2(t) + 0.5\cos(t) - 0.1\sin^2(t)\cos(t) + \sin^5(t)$ is added to the control inputs to excite the system and collect the past data fully.

Figures 3 and 4 show that after 20s, when NN weights converge, the state trajectory of agents 1 and 2 synchronize with the states of the leader while the state trajectory of agent 3 synchronizes with the states of agents 1 and 2. From Fig. 5, it can be seen that the state trajectory of the leader and all agents approach to the origin in finite time. The costs of the leader and agents are presented in Fig. 6, where all signals converge to the near-optimal values.

The control inputs of both ET and TT algorithms, an example of agents 0 and 2, are compared in Figs. 7 and 8. Although the control signals are saturated at the maximum and minimum values, the closed systems are always stable. The control inputs of the time-triggering algorithm are smoother

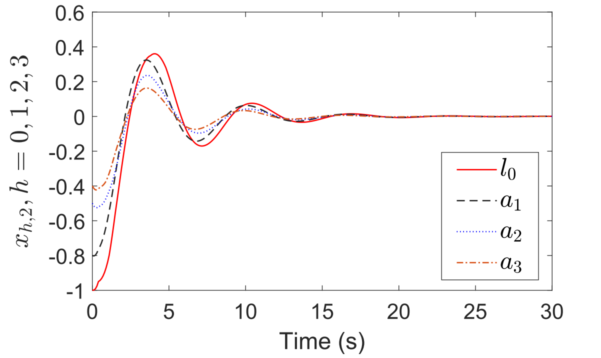

FIGURE 4. Evolution of states of leader and agents for $x_{h,2}, h = 0, \ldots, 3$.

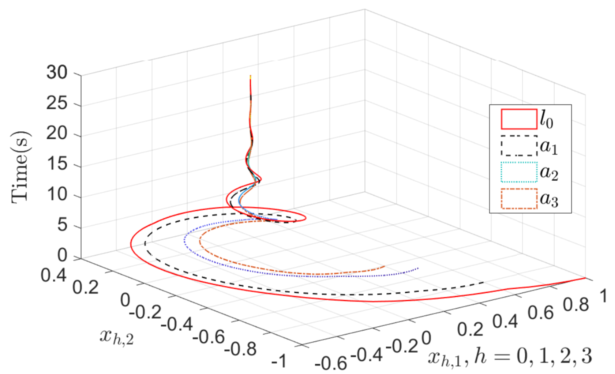

FIGURE 5. 3-D phase plane plot of leader and agents.

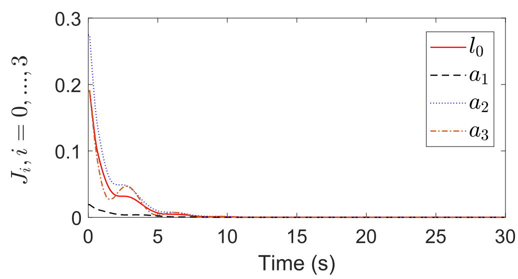

FIGURE 6. Cost functions of leader and agents.

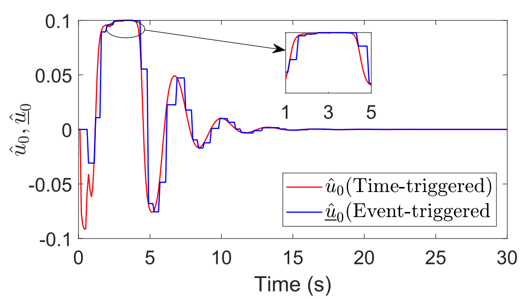

FIGURE 7. Comparison of control inputs between ET and TT of leader.

than those of ET control algorithm over time because the ET control policies do not need to update parameters at each sampling times, and do not generate the control signals,

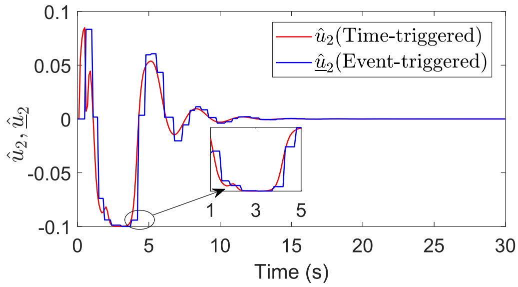

FIGURE 8. Comparison of control inputs between ET and TT of agent 2.

TABLE 1. Communication times for leader and agents.

Algorithms	Leader	Agent 1	Agent 2	Agent 3	Total
Event-triggering	58	58	56	64	236
Time-triggering	300	300	300	300	1200

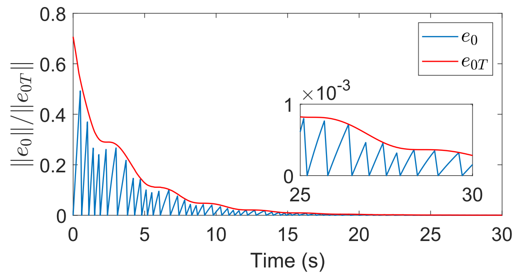

FIGURE 9. Triggering errors and thresholds of leader.

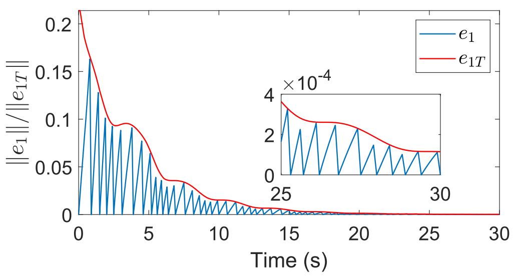

FIGURE 10. Triggering errors and thresholds of agent 1.

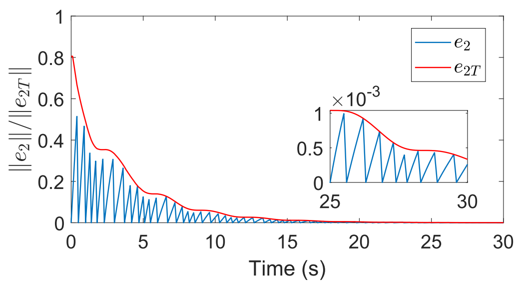

FIGURE 11. Triggering errors and thresholds of agent 2.

which are the same values as previous. Within the inter-event times, the systems are controlled by last triggered control signals.

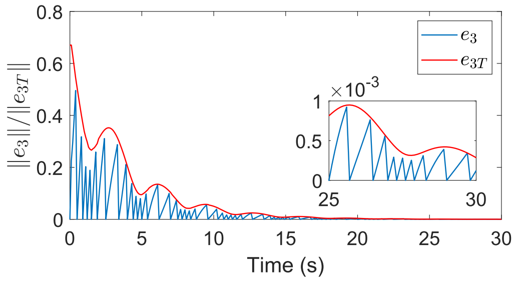

FIGURE 12. Triggering errors and thresholds of agent 3.

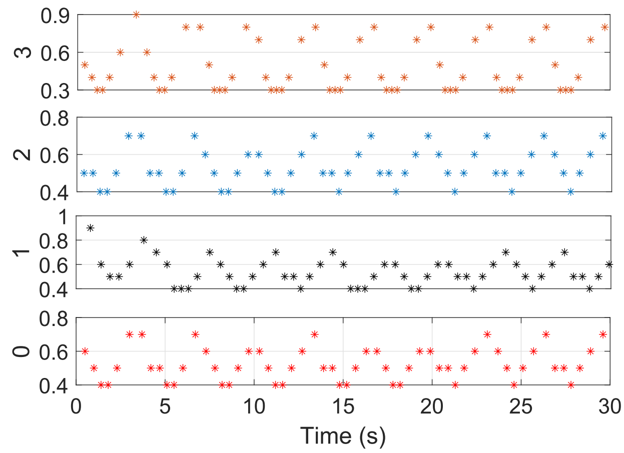

FIGURE 13. Inter-event intervals of leader and agents.

In Figs. 9–12, the thresholds $\|e_{hT}\|, h = 0, 1, 2, 3$ are reduced accordingly the consensus achievement. The triggering errors are less than the thresholds all the time. The inter-event intervals generated by the ET control algorithm is shown in Fig. 13, where the minimum inter-event time is 0.3s. Observing Figs. 9–13 we see that the Zeno phenomenon is excluded.

The effectiveness of reducing burden of communication cost is described in Table 1. The total number of communication times for the event-triggering algorithm is 236 while the total number for the time-triggering algorithm is 1200.

V. CONCLUSION

This paper proposed a method based on the event-triggering signal transmission of the IoT. Such a method is required for the design of the algorithm of distributed H_∞ optimal control for Van der Pol oscillators with unknown internal dynamics, input constraint, and external disturbance. The system dynamics have been transformed into the triggering consensus tracking dynamics, for which the distributed robust optimal control algorithms have been constructed. The algorithm have employed the event-triggering signal transmission of the IoT to reduce the burden of the communication resource and computation bandwidth. As a result, the optimal control policy and disturbance compensation policy have been derived based on the adaptive dynamic programming and two-player zero-sum game theory. The triggering condition has been established such that the Zeno phenomenon is excluded and the stability of the overall closed systems is guaranteed. The numerical simulation results with comparison to the time-triggering algorithms have confirmed the effectiveness of the proposed algorithm. In the future work, we shall concentrate on switching IoT topologies with time-delay.

APPENDIX A
PROOF OF THE THEOREM 1

Proof: Followed by Lemma 1, one only needs to prove the stability of each agent. Note that by setting $\bar{k}_0 = 0$, $x_0 = \delta_i$, and $\underline{x}_0 = \underline{\delta}_i$, it is easy to infer the proof for the leader based on the proof for the agent. First, we propose a Lyapunov function candidate for agent i as

$$L_i = \underbrace{\int_{t-T}^{t} V_i^\star(\delta_i)\mathrm{d}\tau}_{L_{i1}} + \underbrace{\frac{1}{2}\int_{t-T}^{t} \mathrm{trace}\left(\tilde{W}_i^\top \tilde{W}_i\right)\mathrm{d}\tau}_{L_{i2}} + \underbrace{V_i^\star(\underline{\delta}_i)}_{L_{i3}} \tag{33}$$

for the optimal value functions $V_i^\star(\delta_i)$ and $V_i^\star(\underline{\delta}_i)$. We divide the proof into two situations: within the triggering intervals and at the triggering time.

Situation 1:$\dot{L}_{i3}$ is zero as $V_i^\star(\underline{\delta}_i)$ doesn't change within the triggering intervals. Taking the derivative of L_{i1} along (15) and using $\nabla V_i^\star(\delta_{i\vartheta}) f_i$ from (19), we have

$$\dot{L}_{i1} = \int_{t-T}^{t} \dot{V}_i^\star(\delta_{i\vartheta})\mathrm{d}\tau = \int_{t-T}^{t} \nabla V_i^\star(\delta_{i\vartheta})\dot{\delta}_{i\vartheta}\mathrm{d}\tau = \dot{L}_{i1}^i + \dot{L}_{i1}^j \tag{34}$$

where

$$\dot{L}_{i1}^i = \int_{t-T}^{t}\Big(-\delta_i^\top Q_i\delta_i - U(u_i^\star) + \gamma_i^2\|d_i^\star\|^2 - \nabla V_i^{\star\top}\left(\bar{g}_i u_i^\star + \bar{k}_i d_i^\star\right) + \nabla V_i^{\star\top}\left(\bar{g}_i\hat{u}_i + \bar{k}_i\hat{d}_i\right)\Big)\mathrm{d}\tau \tag{35}$$

$$\dot{L}_{i1}^j = \int_{t-T}^{t}\Big(-\sum_{j\in\mathbb{N}_i} a_{ij}U(u_j^\star) + \sum_{j\in\mathbb{N}_i} a_{ij}\gamma_j^2\|d_j^\star\|^2\Big)\mathrm{d}\tau \tag{36}$$

Substituting $u_i^\star$ from (18) to (10), one has

$$U(u_i^\star) = \bar{u}_i(\nabla V_i^\star)^\top \tanh\left(\frac{1}{2\bar{u}_i}R_i^{-1}\bar{g}_i^\top\nabla V_i^\star\right) + \bar{u}_i^2\bar{R}_i \ln\left(\bar{\mathbf{1}} - \tanh^2\left(\frac{1}{2\bar{u}_i}R_i^{-1}\bar{g}_i^\top\nabla V_i^\star\right)\right) \tag{37}$$

where $\bar{R}_i$ is a vector containing main diagonal elements of R_i and $\bar{\mathbf{1}} = [1, 1, 1, 1]^\top$. Replacing (10) into (37) one obtains

$$\dot{L}_{i1}^i = \int_{t-T}^{t}\Big(\nabla V_i^{\star\top}\left(\bar{g}_i(\underline{\hat{u}}_i + \bar{k}_i\underline{\hat{d}}_i - \bar{k}_i d_i^\star\right) - \delta_i^\top Q_i\delta_i + \gamma_i^2\|\underline{d}_i^\star\|^2 - \bar{u}_i^2\bar{R}_i\ln\left(\bar{\mathbf{1}} - \tanh^2(M_i^\star)\right)\Big)\mathrm{d}\tau \tag{38}$$

We change the last term in (38) to

$$\begin{aligned}\bar{u}_i\bar{R}_i\ln\left(\bar{\mathbf{1}} - \tanh^2(M_i^\star)\right) &= \int_{\underline{\hat{u}}_i}^{u_i^\star} 2\bar{u}_i\tanh^{-T}(s/\rho)R\mathrm{d}s \\ &+U(\underline{\hat{u}}_i) - \bar{u}_i\nabla V_i^{\star\top}\bar{g}_i\tanh(M_i^\star)\end{aligned} \tag{39}$$

One can perform the equivalent transformations:

$$\begin{aligned}\nabla V_i^{\star\top}\bar{g}_i\underline{\hat{u}}_i &= \int_{u_i^\star}^{\hat{u}_i} 2\bar{u}_i M_i^{\star\top}R_i\mathrm{d}s - \bar{u}_i\nabla V_i^{\star\top}\bar{g}_i\tanh(M_i^\star),\\ \bar{k}_i^\top\nabla V_i^\star &= 2\gamma_i^2 d_i^{\star\top},\ 2\gamma_i^2 d_i^{\star\top}\underline{\hat{d}}_i \le \gamma_i^2\left(\|d_i^\star\|^2 + \|\underline{\hat{d}}_i\|^2\right),\\ \delta_i^\top Q_i\delta_i &= \underline{\delta}_i^\top Q_i\underline{\delta}_i - 2\underline{\delta}_i^\top Q_i e_i + e_i^\top Q_i e_i\\ &\ge (1-\zeta_i)\lambda_{\min}(Q_i)\|\underline{\delta}_i\|^2 - \left(\frac{1}{\zeta_i} - 1\right)\lambda_{\min}(Q_i)\|e_i\|^2.\end{aligned}$$

Employing the above statements and (39) for (38) we obtain

$$\begin{aligned}\dot{L}_{i1}^i \le \int_{t-T}^{t}\Big(&-(1-\zeta_i)\lambda_{\min}(Q_i)\left\|\underline{\delta}_i\right\|^2 \\ &+\left(\frac{1}{\zeta_i} - 1\right)\lambda_{\min}(Q_i)\|e_i\|^2 - U(\underline{\hat{u}}_i) - \Psi_i + \gamma_i^2\|\underline{\hat{d}}_i\|^2\Big)\mathrm{d}\tau\end{aligned} \tag{40}$$

where

$$\Psi_i = \int_{u_i^\star}^{\hat{u}_i} 2\bar{u}_i\left(\tanh^{-1}(s/\bar{u}_i) + M_i^\star\right)^\top R_i\mathrm{d}s \tag{41}$$

Changing variable $s = -\bar{u}_i\tanh(v)$ one has

$$\begin{aligned}\Psi_i &\le \int_{M_i^\star}^{\underline{\hat{M}}_i} 2\bar{u}_i^2\left(v_i - M_i^\star\right)^\top R_i\mathrm{d}v\\ &= \bar{u}_i^2\left(\underline{\hat{M}}_i - M_i^\star\right)^\top R_i\left(\underline{\hat{M}}_i - M_i^\star\right)\\ &\le \bar{u}_i^2\|R_i\|\|\underline{\hat{M}}_i - M_i^\star\|^2\end{aligned} \tag{42}$$

Using $\nabla V_i^\star$ from (20) for $M_i^\star$ and changing $M_i^\star$ and $\underline{\hat{M}}_i$ in (42) by (25) one yields

$$\begin{aligned}\Psi_i \le \frac{1}{2}\bar{u}_i^2\|R_i^{-1}\|\Big(&\left\|\bar{g}_i^\top\nabla\phi_i^\top(\underline{\delta}_i) - \bar{g}_i^\top\nabla\phi_i^\top(\delta_i)\right\|^2\left\|\hat{W}_i\right\|^2\\ &+\left\|\bar{g}_i^\top\nabla\phi_i^\top(\delta_i)\left(\tilde{W}_i + \nabla\varepsilon(\delta_i)\right)\right\|^2\Big)\end{aligned} \tag{43}$$

Employing the inequality $(xy-uv)^2 \le 2x^2(y-v)^2 + 2v^2(x-u)^2$ and Assumptions 1 and 2 one obtains

$$\left\|\bar{g}_i^\top(\underline{q}_i)\nabla\phi^\top(\underline{\delta}_i) - \bar{g}_i^\top(q_i)\nabla\phi_i^\top(\delta_i)\right\|^2 \le b_{ig}^2 L_{i\nabla\phi}^2\|e_i\|^2 \tag{44}$$

Replacing (43), (44) to (40) one yields

$$\begin{aligned}\dot{L}_{i1}^i \le \int_{t-T}^{t}\Big(&-(1-\zeta_i)\lambda_{\min}(Q_i)\left\|\underline{\delta}_i\right\|^2 - U(\underline{\hat{u}}_i)\\ &+\gamma_i^2\|\underline{\hat{d}}_i\|^2 + \left(\left(\frac{1}{\zeta_i} - 1\right)\lambda_{\min}(Q_i) + \Lambda_i^2\|\hat{W}_i\|^2\right)\|e_i\|^2\\ &+\mu_1\|\tilde{W}_i\|^2 + \mu_2\|\tilde{W}_i\| + \mu_0\Big)\mathrm{d}\tau\end{aligned} \tag{45}$$

where $\Lambda_i^2 = \chi_i L_{i\nabla\phi}^2$, $\chi_i = \frac{1}{2}\bar{u}_i^2 b_{ig}^2 \|R_i^{-1}\|$, $\mu_1 = \chi_i b_{i\nabla\phi}^2$, $\mu_2 = 2\chi_i b_{i\nabla\phi}^2 b_{i\nabla\varepsilon}$, $\mu_0 = \chi b_{i\nabla\phi}^2 b_{i\nabla\varepsilon}^2$.

Next, according to (10) one has

$$U(u_j^\star) = \int_{\hat{\underline{u}}_j}^{u_j^\star} 2\bar{u}_j \tanh^{-\top}(s/\bar{u}_j) R_j \mathrm{d}s + 2U(\hat{\underline{u}}_j) - U(\hat{\underline{u}}_j) \tag{46}$$

where $\beta_1 = \int_{\hat{\underline{u}}_j}^{u_j^\star} 2\bar{u}_j \tanh^{-\top}(s/\bar{u}_j) R_j \mathrm{d}s$ is transformed as

$$\begin{aligned}\beta_1 \le & -\bar{u}_j (W_j - \tilde{W}_i)^\top \nabla\phi_j \bar{g}_j \tanh(\hat{\underline{M}}_j) \\ & + \bar{u}_j (\nabla\phi_j W_j + \nabla\varepsilon_j)^\top \nabla\phi_j \bar{g}_j \tanh(M_j^*) \\ & + \bar{u}_j^2 \bar{R}_j \Big(\ln(1 - \tanh^2(\hat{\underline{M}}_j)) - \ln(1 - \tanh^2(M_j^*)) \Big)\end{aligned} \tag{47}$$

In the fact that $\|\tanh(v)\| \le 1, \forall v$, $\ln(v) \le 1 - v$, $-1 \le \forall v \le 1$, then $\bar{u}_j^2 \bar{R}_j (\ln(1 - \tanh^2(\hat{M}_j)) - \ln(1 - \tanh^2(M_j^*))) \le \beta_2$, where β_2 is a positive constant. Using Assumptions 2 and (47) we have

$$\beta_1 \le \beta_3 \|\tilde{W}_j\| + \beta_4 \tag{48}$$

where $\beta_3 = \bar{u}_j b_{jW} b_{j\nabla\phi} b_{jg}$, $\beta_4 = \bar{u}_j b_{j\nabla\varepsilon} b_{j\nabla\phi} b_{jg} + 2\beta_3 + \beta_2$. It can be seen that from (46) $2\|U(\hat{\underline{u}}_j)\| \le \beta_5$ and by changing $s = -\bar{u}_j \tanh(\nu)$, $-U(\hat{\underline{u}}_j)$ becomes

$$\begin{aligned}-U(\hat{\underline{u}}_j) &= \int_{\hat{\underline{u}}_j}^{0} 2\bar{u}_j \tanh^{-\top}(s/\bar{u}_j) R_j \mathrm{d}s \\ &\le \int_{\hat{\underline{u}}_j}^{0} 2\bar{u}_j^2 R_j \nu \mathrm{d}\nu \le -\frac{1}{4}\beta_6 \|\tilde{W}_j\|^2 + \frac{1}{2}\beta_7 \|\tilde{W}_j\|\end{aligned} \tag{49}$$

where $\beta_6 = b_{j\nabla\phi}^2 \min_{j\in\mathbb{N}_i}(b_{jR})$, $\lambda_7 = b_{j\nabla\phi}^2 \max_{j\in\mathbb{N}_i}(b_{jR})$, $b_{jR} = \|R_j^{-1}\| b_{jg}^2$. By replacing (47) and (49) to (46), then using the result for (36) one yields

$$\dot{L}_{i1}^j \le -\sum_{j\in\mathbb{N}_i} \left(\frac{1}{4}\beta_6 \|\tilde{W}_j\|^2 - \beta_8 \|\tilde{W}_j\| \right) + \beta_4 \tag{50}$$

where $\beta_8 = \beta_3 + \frac{1}{2}\beta_7$.

On the other hand, taking differential L_{i2} along (28), we have

$$\begin{aligned}\dot{L}_{i2} = \int_{t-T}^{t} \bigg(& -\alpha \tilde{W}_i^\top \Omega_i \tilde{W}_i \\ & + \alpha \tilde{W}_i^\top \Big(\Delta\phi_i \varepsilon_{iH} + \sum_{l=1}^{P_i} \Delta\phi_i(t_l) \varepsilon_{iH}(t_l) \Big) \bigg) \mathrm{d}\tau\end{aligned} \tag{51}$$

where $\Omega_i = \Delta\phi_i \Delta\phi_i^\top + \sum_{l=1}^{P_i} \Delta\phi_i(t_l) \Delta\phi_i(t_l)^\top$, $\Omega_i > 0$. Using the Young's inequality and the upper bound of $\varepsilon_{iH}(.)$, The last term of (51) becomes

$$\begin{aligned}\dot{L}_{i2} \le & -(\rho_i - 1)\lambda_{\min}(\Omega_i) \int_{t-T}^{t} \left\| \tilde{W}_i \right\|^2 \mathrm{d}\tau \\ & + \frac{\rho_i^2}{4}(P_i + 1) \int_{t-T}^{t} b_{i\varepsilon H}^2 \mathrm{d}\tau\end{aligned} \tag{52}$$

Substituting (52) and (45) to (33) yields

$$\begin{aligned}\dot{L}_i \le \int_{t-T}^{t} \Bigg(& -(1-\zeta_i)\lambda_{\min}(Q_i) \left\| \underline{\delta}_i \right\|^2 - U(\hat{\underline{u}}_i) \\ & + \bigg(\Big(\frac{1}{\zeta_i} - 1 \Big) \lambda_{\min}(Q_i) + \Lambda_i^2 \|\hat{W}_i\|^2 \bigg) \|e_i\|^2 \\ & + \gamma_i^2 \|\hat{\underline{d}}_i\|^2 - \mu_3 \Big(\|\tilde{W}_i\| - \frac{\mu_2}{2\mu_3} \Big)^2 \\ & - \sum_{j\in\mathbb{N}_i} \beta_6 \Big(\frac{1}{2} \|\tilde{W}_j\| - \frac{\beta_8}{\beta_6} \Big)^2 + \mu_4 \Bigg) \mathrm{d}\tau\end{aligned} \tag{53}$$

where $\mu_3 = \rho_i - \mu_1 - 1$. $\mu_3 > 0$. If the convergence rate is chosen $\rho_i > \mu_1 + 1$. $\mu_4 = \mu_0 + \frac{\rho_i^2}{4}(P_i + 1) b_{i\varepsilon H}^2 + \frac{\mu_2^2}{4\mu_3} + \beta_4 + \frac{\beta_8^2}{\beta_6}$. Define $b_{i\tilde{W}} = \sqrt{\mu_4/\mu_3} + \frac{\mu_2}{2\mu_3}$, $b_{j\tilde{W}} = \sqrt{\mu_4/\beta_6} + \frac{\beta_8}{\beta_6}$, noting the triggering condition (31) and when $\|\tilde{W}_i\| > b_{i\tilde{W}}$ or $\frac{1}{2}\sum_{j\in\mathbb{N}_i} \|\tilde{W}_j\| > b_{j\tilde{W}}$, we have $\dot{L}_i < -\frac{1}{T}\beta((1-\zeta_i)\lambda_{\min}(Q_i)\left\|\underline{\delta}_i\right\|^2 + U(\hat{\underline{u}}_i) - \gamma_i^2 \|\hat{\underline{d}}_i\|^2) < 0, \forall t$. Therefore, by Definition 1, the consensus NN approximation errors are UUB and the closed dynamics guarantees to be asymptotically stable. Note that by choosing ρ_i appropriately, the approximation errors will be asymptotic to arbitrarily small values.

Situation 2: $\forall t = t_k^i$, $\forall k \in \mathbb{N}$, taking the difference of (33) one obtains

$$\begin{aligned}\Delta L_i = & V_i^\star(\underline{\delta}_i(t_k^i)) - V_i^\star(\underline{\delta}_i(t_{k-1}^i)) \\ & + \int_{t_k^i - T}^{t_k^i} V^\star(\underline{\delta}_i) \mathrm{d}\tau - \int_{t_k^{i-} - T}^{t_k^{i-}} V_i^\star(\delta_i(t^-)) \mathrm{d}\tau \\ & + \frac{1}{2}\tilde{W}_i^\top(t_k^i)\tilde{W}_i(t_k^i) - \frac{1}{2}\tilde{W}_i^\top(t^-)\tilde{W}_i(t^-)\end{aligned} \tag{54}$$

From (53), as $\dot{L}_i < 0$ and the trajectories of (28) and (15) are continuous, we have

$$\int_{t_k^i - T}^{t_k^i} V_i^\star(\underline{\delta}_i(t_k^i)) \mathrm{d}\tau \le \int_{t_k^{i-} - T}^{t_k^{i-}} V_i^\star(\delta_i(t^-)) \mathrm{d}\tau \tag{55}$$

$$\tilde{W}_i^\top(t_k^i)\tilde{W}_i(t_k^i) \le \tilde{W}_i^\top(t^-)\tilde{W}_i(t^-) \tag{56}$$

Then, we rewrite ΔL_i as

$$\begin{aligned}\Delta L_i &\le V_i^\star(\underline{\delta}_i(t_k^i)) - V^\star(\underline{\delta}_i(t_{k-1}^i)) \\ &\le V_i^\star(\delta_i(t^-)) - V_i^\star(\underline{\delta}_i(t_{k-1}^i)) \\ &\le -\kappa_i \|\delta_i(t^-) - \underline{\delta}_i(t_{k-1}^i)\| = -\kappa_i \|e_i(t_{k-1}^i)\|\end{aligned} \tag{57}$$

where κ_i is in a class-κ function [41]. Recalling (54), it can be seen that the Lyapunov function (33) it is continuously reducing at any triggering time, $t = t_k^i$, $k \in \mathbb{N}$.

From (53) and (57), it can be included that the closed dynamics has been asymptotically stable.

To prove the Zeno behavior is excluded, we observe (24), (25) and Lipschitz property of $f_i(\underline{z}_i)$. The dynamics (15), $\forall t \in [t_k^i, t_{k+1}^i)$, satisfies

$$\left\| \dot{\delta}_i \right\| \le b_{if} \left\| \delta_i \right\| + \Gamma_{i0} \left\| \hat{W}_i \right\| \left\| \underline{\delta}_i \right\| \tag{58}$$

where $\Gamma_{i0} = \|R_i^{-1}\|/2b_{ig}^2 L_{i\nabla\delta_i} + b_{ik}^2/(2\gamma_i^2) L_{i\nabla\delta_i}, f_i \le b_{if}\|\delta_i\|$, $b_{if} > 0$. For a small positive real number a_i, we have

$$\left\|\dot{e}_i\right\| \le \Gamma_i \left\|e_i\right\| + \Gamma_i\left(\left\|\underline{\delta}_i\right\| + a_i\right) \tag{59}$$

where $\Gamma_i = \Gamma_{i0} + b_{if}$. Formally, we can follow from [43] to prove the rest of the proof.

This completes the proof. ■

REFERENCES

[1] N. Gupta, Ed., *Human-Machine Interaction and IoT Applications for a Smarter World*, 1st ed. Boca Raton, FL, USA: CRC Press, 2022.
[2] M. Bouzidi, N. Gupta, F. A. Cheikh, A. Shalaginov, and M. Derawi, "A novel architectural framework on IoT ecosystem, security aspects and mechanisms: A comprehensive survey," *IEEE Access*, vol. 10, pp. 101362–101384, 2022.
[3] M. M. Rana, W. Xiang, E. Wang, X. Li, and B. J. Choi, "Internet of Things infrastructure for wireless power transfer systems," *IEEE Access*, vol. 6, pp. 19295–19303, 2018.
[4] W. Ali, A. Ulasyar, M. U. Mehmood, A. Khattak, K. Imran, H. S. Zad, and S. Nisar, "Hierarchical control of microgrid using IoT and machine learning based islanding detection," *IEEE Access*, vol. 9, pp. 103019–103031, 2021.
[5] W. Fei, H. Ni, and W. Yan, "Application of discrete event-triggered H_∞ control in wireless signal transmission of IoT," *J. Supercomput.*, vol. 77, no. 6, pp. 6251–6272, Jun. 2021.
[6] A. Saad, S. Faddel, T. Youssef, and O. A. Mohammed, "On the implementation of IoT-based digital twin for networked microgrids resiliency against cyber attacks," *IEEE Trans. Smart Grid*, vol. 11, no. 6, pp. 5138–5150, Nov. 2020.
[7] P. Kolios, C. Panayiotou, G. Ellinas, and M. Polycarpou, "Data-driven event triggering for IoT applications," *IEEE Internet Things J.*, vol. 3, no. 6, pp. 1146–1158, Dec. 2016.
[8] G. M. Milis, C. G. Panayiotou, and M. M. Polycarpou, "IoT-enabled automatic synthesis of distributed feedback control schemes in smart buildings," *IEEE Internet Things J.*, vol. 8, no. 4, pp. 2615–2626, Feb. 2021.
[9] M. Lemmon, "Event-triggered feedback in control, estimation, and optimization," in *Networked Control Systems* (Lecture Notes in Control and Information Sciences), vol. 406, A. Bemporad, M. Heemels, and M. Johansson, Eds. London, U.K.: Springer, 2010.
[10] P. Tabuada, "Event-triggered real-time scheduling of stabilizing control tasks," *IEEE Trans. Autom. Control*, vol. 52, no. 9, pp. 1680–1685, Sep. 2007.
[11] V. Narayanan, H. Modares, and S. Jagannathan, "Event-triggered control of input-affine nonlinear interconnected systems using multiplayer game," *Int. J. Robust Nonlinear Control*, vol. 31, no. 3, pp. 950–970, Feb. 2021.
[12] V. Narayanan and S. Jagannathan, "Event-triggered distributed approximate optimal state and output control of affine nonlinear interconnected systems," *IEEE Trans. Neural Netw. Learn. Syst.*, vol. 29, no. 7, pp. 2846–2856, Jul. 2018.
[13] K. G. Vamvoudakis, A. Mojoodi, and H. Ferraz, "Event-triggered optimal tracking control of nonlinear systems," *Int. J. Robust Nonlinear Control*, vol. 27, no. 4, pp. 598–619, Mar. 2017.
[14] L. N. Tan, "Event-triggered distributed H_∞ constrained control of physically interconnected large-scale partially unknown strict-feedback systems," *IEEE Trans. Syst., Man, Cybern., Syst.*, vol. 51, no. 4, pp. 2444–2456, Apr. 2021.
[15] C. Qin, H. Zhu, J. Wang, Q. Xiao, and D. Zhang, "Event-triggered safe control for the zero-sum game of nonlinear safety-critical systems with input saturation," *IEEE Access*, vol. 10, pp. 40324–40337, 2022.
[16] K. G. Vamvoudakis, F. R. Pour Safaei, and J. P. Hespanha, "Robust event-triggered output feedback learning algorithm for voltage source inverters with unknown load and parameter variations," *Int. J. Robust Nonlinear Control*, vol. 29, no. 11, pp. 3502–3517, Jul. 2019.
[17] C. Nowzari, E. Garcia, and J. Cortés, "Event-triggered communication and control of networked systems for multi-agent consensus," *Automatica*, vol. 105, pp. 1–27, Jul. 2019.
[18] B. van der Pol, "VII. Forced oscillations in a circuit with non-linear resistance. (Reception with reactive triode)," *London, Edinburgh, Dublin Phil. Mag. J. Sci.*, vol. 3, no. 13, pp. 65–80, Jan. 1927.
[19] C. Gong, F. Lin, and X. An, "A novel emotion control system for embedded human–computer interaction in green IoT," *IEEE Access*, vol. 7, pp. 185148–185156, 2019.
[20] W. M. Haddad and V. Chellaboina, *Nonlinear Dynamical Systems and Control: A Lyapunov-Based Approach*. Princeton, NJ, USA: Princeton Univ. Press, 2008.
[21] S. H. Strogatz, *Nonlinear Dynamics and Chaos: With Applications to Physics, Biology, Chemistry, and Engineering*, 1st ed. Boulder, CO, USA: Westview, 2014.
[22] F. Veerman and F. Verhulst, "Quasiperiodic phenomena in the van der Pol–Mathieu equation," *J. Sound Vib.*, vol. 326, nos. 1–2, pp. 314–320, Sep. 2009.
[23] B. van der Pol, "The nonlinear theory of electric oscillations," *Proc. Inst. Radio Eng.*, vol. 22, no. 9, pp. 1051–1086, Sep. 1934.
[24] A. J. Calise, N. Hovakimyan, and M. Idan, "Adaptive output feedback control of nonlinear systems using neural networks," *Automatica*, vol. 37, no. 8, pp. 1201–1211, Aug. 2001.
[25] A. Loría, E. Panteley, and H. Nijmeijer, "A remark on passivity-based and discontinuous control of uncertain nonlinear systems," *Automatica*, vol. 37, no. 9, pp. 1481–1487, Sep. 2001.
[26] N. Hovakimyan, F. Nardi, A. Calise, and N. Kim, "Adaptive output feedback control of uncertain nonlinear systems using single-hidden-layer neural networks," *IEEE Trans. Neural Netw.*, vol. 13, no. 6, pp. 1420–1431, Nov. 2002.
[27] A. Yeşildirek and F. L. Lewis, "Feedback linearization using neural networks," *Automatica*, vol. 31, no. 11, pp. 1659–1664, 1995.
[28] H. Ahmed, H. Ríos, B. Ayalew, and Y. Wang, "Second-order sliding-mode differentiators: An experimental comparative analysis using Van der Pol oscillator," *Int. J. Control*, vol. 91, no. 9, pp. 2100–2112, Sep. 2018.
[29] W. Gao and Z.-P. Jiang, "Learning-based adaptive optimal tracking control of strict-feedback nonlinear systems," *IEEE Trans. Neural Netw. Learn. Syst.*, vol. 29, no. 6, pp. 2614–2624, Jun. 2018.
[30] S. Tong, K. Sun, and S. Sui, "Observer-based adaptive fuzzy decentralized optimal control design for strict-feedback nonlinear large-scale systems," *IEEE Trans. Fuzzy Syst.*, vol. 26, no. 2, pp. 569–584, Apr. 2018.
[31] K. G. Vamvoudakis, M. F. Miranda, and J. P. Hespanha, "Asymptotically stable adaptive-optimal control algorithm with saturating actuators and relaxed persistence of excitation," *IEEE Trans. Neural Netw. Learn. Syst.*, vol. 27, no. 11, pp. 2386–2398, Nov. 2016.
[32] L. N. Tan, "Omnidirectional-vision-based distributed optimal tracking control for mobile multirobot systems with kinematic and dynamic disturbance rejection," *IEEE Trans. Ind. Electron.*, vol. 65, no. 7, pp. 5693–5703, Jul. 2018.
[33] L. N. Tan, "Distributed H_∞ optimal tracking control for strict-feedback nonlinear large-scale systems with disturbances and saturating actuators," *IEEE Trans. Syst., Man, Cybern. Syst.*, vol. 50, no. 11, pp. 4719–4731, Nov. 2020.
[34] P. Ioannou and J. Sun, *Robust Adaptive Control*. Upper Saddle River, NJ, USA: Prentice-Hall, 1996.
[35] A. Das and F. L. Lewis, "Distributed adaptive control for synchronization of unknown nonlinear networked systems," *Automatica*, vol. 46, no. 12, pp. 2014–2021, 2010.
[36] M. Abu-Khalaf and F. L. Lewis, "Nearly optimal control laws for nonlinear systems with saturating actuators using a neural network HJB approach," *Automatica*, vol. 41, no. 5, pp. 779–791, May 2005.
[37] A. J. van der Schaft, "$\mathcal{L}_2$-gain analysis of nonlinear systems and nonlinear state-feedback H_∞ control," *IEEE Trans. Autom. Control*, vol. 37, no. 6, pp. 770–784, Jun. 1992.
[38] Q. Jiao, H. Modares, S. Xu, F. L. Lewis, and K. G. Vamvoudakis, "Multi-agent zero-sum differential graphical games for disturbance rejection in distributed control," *Automatica*, vol. 69, pp. 24–34, Jul. 2016.
[39] K. G. Vamvoudakis and F. L. Lewis, "Online solution of nonlinear two-player zero-sum games using synchronous policy iteration," *Int. J. Robust Nonlinear Control*, vol. 22, no. 13, pp. 1460–1483, 2012.
[40] D. Vrabie and F. Lewis, "Neural network approach to continuous-time direct adaptive optimal control for partially unknown nonlinear systems," *Neural Netw.*, vol. 22, no. 3, pp. 237–246, 2009.

[41] H. K. Khalil, *Nonlinear Systems*, 3rd ed. Englewood Cliffs, NJ, USA: Prentice-Hall, 2002.
[42] G. Chowdhary and E. Johnson, "Concurrent learning for convergence in adaptive control without persistency of excitation," in *Proc. 49th IEEE Conf. Decis. Control (CDC)*, Dec. 2010, pp. 3674–3679.
[43] Q. Zhang, D. Zhao, and Y. Zhu, "Event-triggered H_∞ control for continuous-time nonlinear system via concurrent learning," *IEEE Trans. Syst., Man, Cybern., Syst.*, vol. 47, no. 7, pp. 1071–1081, Jul. 2016.

LUY NGUYEN TAN (Member, IEEE) received the B.S. and M.Sc. degrees in computer science and automation and control engineering and the Ph.D. degree in automation from the Ho Chi Minh City University of Technology, Vietnam, in 1996, 2006, and 2015, respectively. He is currently with the Faculty of Electrical-Electronics Engineering (FEEE), HCMUT, Vietnam National University Ho Chi Minh City (VNU-HCM), Vietnam. His current research interests include adaptive dynamic programming, distributed control, large-scale systems, and deep learning.

He served as a Reviewer for many journals, including IEEE Transactions on Neural Network and Learning Systems, IEEE Transactions on Industrial Electronics, IEEE Transactions on Industrial Informatics, IEEE Transactions on Cybernetics, IEEE Transactions on Systems, Man Cybernetics—Part A: Systems, and IEEE Access (Elsevier).

NISHU GUPTA (Senior Member, IEEE) received the Ph.D. degree in electronics and communication engineering from MNNIT Allahabad, Prayagraj, India, in 2016. He is currently a Postdoctoral Fellow (ERCIM Alain Bensoussan Fellowship) with the Department of Electronic Systems, Faculty of Information Technology and Electrical Engineering, Norwegian University of Science and Technology (NTNU), Gjøvik, Norway. He has served as a member of Zero Trust Architecture working group of MeitY-C-DAC-STQC Project under "e-Governance Standards and Guidelines," Ministry of Electronics and Information Technology (MeitY), Government of India. Recently, he won the Electronics, MDPI Travel Grant Award for the year 2022. He is specialized in the field of computer communication and networking. His major work is in the area of IoT-based enhanced safety applications in vehicular communication. He is the author and editor of several books and book chapters with publishers, including Springer, Taylor & Francis, Wiley, and Scrivener publishing. His research interests include intelligent vehicles, the Internet of Things, smart city and transportation, augmented cyber-security, vehicular communication, driving behavior analysis, ADAS, and security in sensor networks. He was a recipient of Best Paper Presentation Award at NTU, Singapore, in 2019, and he serves as a reviewer of various high quality journals.

MOHAMMAD DERAWI received the Diploma degree in computer science engineering from the Technical University of Denmark (DTU), Denmark, the B.Sc. and M.Sc. degrees from DTU, in 2007 and 2009, respectively, and the joint Ph.D. degree in information security from the Norwegian Information Security Laboratory (NISLaboratory), NTNU, and the Center for Advanced Security Research Darmstadt (CASED), Germany (www.cased.de). He is currently having a dual-career acting as the Youngest Professor of Norway and an Extremely True Innovator. In addition, he received the title as the Youngest Engineer of Denmark, in 2009, and the Youngest Full Professor in Nordics, in 2017. He has been active in several European and national projects, since 2009. He holds a professorship within electrical engineering and is specialized within information security, e-health, autonomous systems, biometric systems, wireless communications, the IoT, digital fundamentals, and microcontrollers. He is also the Head of the "Smart Wireless Systems" Research Group, Department of Electronic Systems (NTNU), Gjøvik, Norway, where he is the Scientific Director of the IoT-Laboratory. He has next to his academic career also been working with truly innovative projects which is also a part of his additional skills, where he also identifies the need within an industry, market segment or culture, and spot opportunity in it. More importantly, he has also the ability to identify needs before implemented in the market, develop and refine solutions, take chances, push the envelope, and create meaning.